Air-sea interactions during the passage of a winter storm over the Gulf Stream: A three-dimensional coupled atmosphere-ocean model study

Yongping Li[1] and Huijie Xue
School of Marine Sciences, University of Maine, Orono, Maine, USA

John M. Bane
Department of Marine Sciences, University of North Carolina, Chapel Hill, North Carolina, USA

Received 1 October 2001; revised 16 May 2002; accepted 13 August 2002; published 21 November 2002.

[1] A three-dimensional, regional coupled atmosphere-ocean model with full physics is developed to study air-sea interactions during winter storms off the U. S. east coast. Because of the scarcity of open ocean observations, models such as this offer valuable opportunities to investigate how oceanic forcing drives atmospheric circulation and vice versa. The study presented here considers conditions of strong atmospheric forcing (high wind speeds) and strong oceanic forcing (significant sea surface temperature (SST) gradients). A simulated atmospheric cyclone evolves in a manner consistent with Eta reanalysis, and the simulated air-sea heat and momentum exchanges strongly affect the circulations in both the atmosphere and the ocean. For the simulated cyclone of 19–20 January 1998, maximum ocean-to-atmosphere heat fluxes first appear over the Gulf Stream in the South Atlantic Bight, and this results in rapid deepening of the cyclone off the Carolina coast. As the cyclone moves eastward, the heat flux maximum shifts into the region near Cape Hatteras and later northeast of Hatteras, where it enhances the wind locally. The oceanic response to the atmospheric forcing is closely related to the wind direction. Southerly and southwesterly winds tend to strengthen surface currents in the Gulf Stream, whereas northeasterly winds weaken the surface currents in the Gulf Stream and generate southwestward flows on the shelf. The oceanic feedback to the atmosphere moderates the cyclone strength. Compared with a simulation in which the oceanic model always passes the initial SST to the atmospheric model, the coupled simulation in which the oceanic model passes the evolving SST to the atmospheric model produces higher ocean-to-atmosphere heat flux near Gulf Stream meander troughs. This is due to wind-driven lateral shifts of the stream, which in turn enhance the local northeasterly winds. Away from the Gulf Stream the coupled simulation produces surface winds that are 5 $\sim$ 10% weaker. Differences in the surface ocean currents between these two experiments are significant on the shelf and in the open ocean. *INDEX TERMS:* 4255 Oceanography: General: Numerical modeling; 4504 Oceanography: Physical: Air/sea interactions (0312); 4528 Oceanography: Physical: Fronts and jets; 4576 Oceanography: Physical: Western boundary currents; *KEYWORDS:* coupled model, winter storm, Gulf Stream, air-sea interaction

Citation: Li, Y., H. Xue, and J. M. Bane, Air-sea interactions during the passage of a winter storm over the Gulf Stream: A three-dimensional coupled atmosphere-ocean model study, *J. Geophys. Res.*, *107*(C11), 3200, doi:10.1029/2001JC001161, 2002.

1. Introduction

[2] Making accurate coastal weather and marine predictions during winter storms remains a challenging problem in meteorology and oceanography. Progress is hindered by incomplete understanding of air-sea interaction processes, compounded by the lack of fine resolution coastal and open ocean observations. Three field programs conducted in late 1980s, the Genesis of Atlantic Low Experiment (GALE) [*Blanton et al.*, 1987; *Dirks et al.*, 1988], the Canadian Atlantic Storms Program (CASP) [*Stewart et al.*, 1987], and the Experiment on Rapid Intensifying Cyclones over the Atlantic (ERICA) [*Hadlock and Kreitzberg*, 1988] emphasized the role of excessive heat fluxes from the ocean, particularly the Gulf Stream, in the development of winter marine cyclones in the northwest Atlantic. Of these three programs, only GALE collected concurrent atmospheric and oceanic data in the Gulf Stream and shelf waters of the South Atlantic Bight (SAB) [*Blanton et al.*, 1987]. The observations of the Gulf Stream did not include current measurements, and so much of our present understanding of

[1]Now at Shanghai Typhoon Institute, Shanghai, China.

0148-0227/02/2001JC001161

the response of the Gulf Stream's currents to winter storms derives from numerical studies [*Ademec and Elsberry*, 1985a, 1985b; *Chao*, 1992; *H. Xue et al.*, 1995, 2000]. More studies are needed to examine the role of air-sea interactions in the Mid-Atlantic Bight (MAB) and in the offshore extension of the Gulf Stream.

[3] A mesoscale atmospheric model coupled with a regional oceanic model is a useful tool for the study of coastal weather and marine cyclones. Coupled models describe the feedback between the atmosphere and ocean which is important to storm development. For example, the effect of the atmospherically forced sea state variation on the atmospheric boundary layer and the effect of oceanically forced atmospheric variation on the upper ocean can be addressed. Coupled- model studies of the response of the Gulf Stream to strong atmospheric forcing include *Chao* [1992] and *Xue et al.* [2000]. *Chao* [1992] coupled a two-dimensional, dry atmospheric model with a two-dimensional oceanic model to investigate how an atmospheric cold front interacts with the Gulf Stream and its adjacent waters. The dry atmosphere in this model excluded the mechanism of latent heating, which has been shown to be a dominant forcing in the development of mesoscale structures in the marine atmospheric boundary layer (MABL) [*Warner et al.*, 1990; *Reed et al.*, 1993]. *Xue et al.* [2000] used a two-dimensional coupled model with full physics to study air-sea interaction processes during an extreme cold air outbreak over the Gulf Stream off the southeastern U.S.

[4] Variations along the Gulf Stream were not addressed in these two-dimensional simulations. As well, both studies focused on the cold air outbreak phase of a passing atmospheric cyclone. However, the cold air portion is only one component of an extratropical cyclone system, which usually contains both a cold front and a warm front. Winds can change rapidly in direction and magnitude as a storm progresses past a fixed location [*Sanders and Gyakum*, 1980]. Air temperature and humidity vary according to the prevailing wind directions, and so air-sea exchanges at different positions and phases of the progressing storm are expected to differ greatly. In the SAB, the storm-associated cold front typically extends from the storm center toward the southwest, roughly parallel to the coastline and the Gulf Stream. Air-sea fluxes in the SAB thus tend to have large gradients in the cross-stream direction but small gradients in the alongstream direction [*Blanton et al.*, 1989]. A cold front sweeps across the Gulf Stream in a relatively short period of time, and this typically results in rapid temporal changes in air-sea fluxes at any fixed location.

[5] In contrast to their behavior in the SAB, storms typically move parallel to the Gulf Stream downstream of Cape Hatteras. Because air masses on either side of the cold front differ significantly, gradients of air-sea fluxes along the Gulf Stream are expected to be large. Furthermore, the oceanic response to storm forcing depends largely on the specific cyclone path. *Beardsley and Butman* [1974] observed a large alongshore sea level gradient and large current oscillations during westerly winds, in contrast to large sea level increases at coastal stations with little alongshore sea level gradient and large net westward alongshore currents during northeasterly winds. A more complex shelf circulation may appear in the MAB when the northern MAB is controlled by northeasterlies and the southern MAB by the westerlies, as is typical of maritime storms in winter.

[6] In this paper, a three-dimensional coupled model will simulate atmospheric and oceanic conditions during a typical east coast winter storm. The main objectives of this paper are to (1) gain an increased understanding of the temporal and spatial variations of the air-sea fluxes over the SAB, the MAB and the Gulf Stream east of Cape Hatteras during the passage of a winter storm and (2) demonstrate how sea surface temperature (SST) and Gulf Stream transport respond to the storm in the SAB, off Cape Hatteras and east of Cape Hatteras. The following section introduces the three-dimensional coupled atmosphere-ocean model used in this study. It is followed by discussions on model initialization and boundary conditions, and a synoptic description of the 19–20 January 1998 storm. Section 4 discusses the coupled model results, and section 5 summarizes the study.

2. Model Description

[7] The coupled model consists of three components: an atmospheric model, an oceanic model, and a coupling scheme. The atmospheric model is the Advanced Regional Prediction System (ARPS) developed by the Center for Analysis and Prediction of Storms at the University of Oklahoma. Details of the ARPS are given by *M. Xue et al.* [1995]. Briefly, the ARPS is designed to predict small scale and mesoscale weather events. It is nonhydrostatic, and thus is suitable for simulating the strong convection that usually occurs in rapidly developing storms. The ARPS includes momentum, heat (potential temperature), mass (pressure), six categories of water (water vapor, cloud water, rainwater, cloud ice, snow, and hail), a 1.5-order turbulence kinetic energy (TKE) closure scheme, and the equation of state. All vertical diffusion terms are computed by a time implicit scheme. The model domain of 2400 km $\times$ 2400 km used in this study (Figure 1) covers all U. S. Atlantic coast states and most Canadian maritime provinces, and the northwest corner of the domain extends farther inland to the Great Lakes region. A uniform horizontal resolution of 20 km is used in this study. In the vertical there are 26 terrain-following, stretched levels with higher resolution in the atmospheric planetary boundary layer (Figure 2a). For a typical MABL depth of 1000 m, there are 7 grid points within the MABL. The synoptic and planetary-scale background fields are represented by a time-dependent external boundary condition.

[8] The oceanic model is the Princeton Ocean Model (POM). POM [*Blumberg and Mellor*, 1987] is a three-dimensional, fully nonlinear, primitive equation ocean model. It predicts the following prognostic variables: u and v (horizontal velocities), T (temperature), S (salinity), and η (sea level). Additionally, w (vertical velocity), p (pressure), and ρ (density) are calculated diagnostically using the continuity equation, the hydrostatic relationship and the equation of state. The POM includes the second-order turbulence closure scheme of *Mellor and Yamada* [1982] to calculate turbulence viscosity and diffusivity. In the vertical an implicit scheme permits the use of fine resolution in the surface layers and eliminates time con-

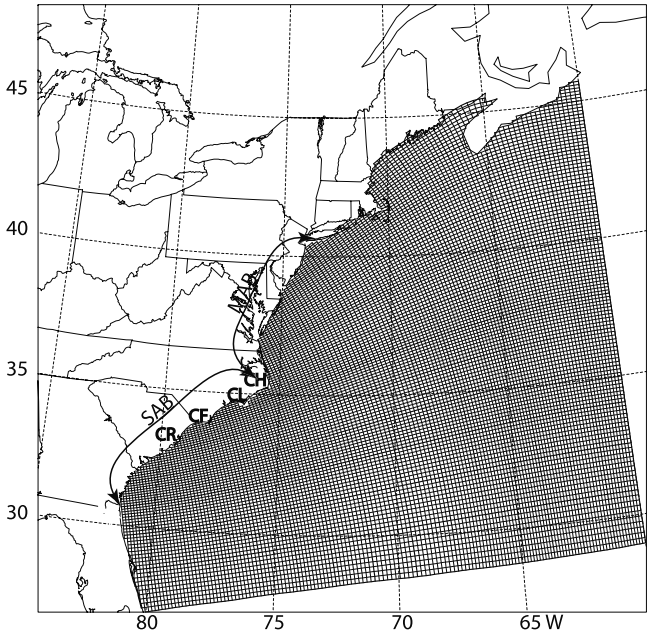

Figure 1. The outer box shows the ARPS domain of 2400 km × 2400 km. A constant resolution of 20 km is used. The mesh shows the POM curvilinear grid used in this study. CR = Cape Romain, CF = Cape Fear, CL = Cape Lookout, CH = Cape Hatteras, SAB = South Atlantic Bight, and MAB = Mid-Atlantic Bight.

straints for the vertical coordinate. The oceanic model domain is shown in Figure 1. It extends well offshore into the open Atlantic Ocean so that the area of interest is far from the model open boundary. An orthogonal curvilinear grid is constructed with 151 × 121 horizontal grid points and about 10 to 15 km resolution in the shelf and the Gulf Stream. In the vertical there are 26 sigma levels with fine resolution in the upper ocean (Figure 2b).

[9] To couple the ARPS with POM, a concurrent process communication technique [*Xue et al.*, 2000] is used to establish the linkage between the two models such that the momentum flux and heat fluxes (including latent heat flux, sensible heat flux, short and long wave radiation fluxes) are passed from the atmospheric model to the oceanic model, and vice versa for SST. ARPS includes a stability and roughness-dependent surface flux model based on the Businger formulation [*Businger et al.*, 1971]. The momentum stress, turbulent heat flux and turbulent moisture flux are calculated using the bulk formulae as functions of the wind at the lowest level, differences of temperature and water vapor mixing ratio between the lowest level and the surface (ground or water surface). The drag and exchange coefficients are Richardson number and surface roughness dependent. Although the oceanic surface wave field is not explicit in the coupled model, the surface roughness length over the ocean is related to the surface wind speed [*M. Xue et al.*, 1995].

[10] The atmospheric model and the oceanic model have different grids in this study. Surface momentum flux and heat fluxes from the atmospheric model need to be spatially interpolated to the oceanic model grid, while SST from the oceanic model needs to be interpolated to the atmospheric model grid. The interpolation is based on a linear rule such that the variables being exchanged over the ocean for any one of the two models are obtained by linear interpolation of the four nearest grids in the other model. Time steps used in this study are 15 s for the APRS and 360 s for the POM (internal), and exchange between the two models occurs on every oceanic model time step.

[11] Atmospheric data, including geopotential height, temperature, u and v wind components and specific humidity on 26 mandatory pressure levels, were obtained from the National Center for Environmental Prediction (NCEP) Eta model regional analysis for the January 1998 study period. The Eta reanalysis is available at 3 hour intervals with a horizontal resolution of about 40 km. These data are used to initialize the atmospheric model, and they are linearly interpolated to provide time-dependent boundary conditions for the atmospheric model at every time step.

[12] Oceanic data, including water temperature, salinity, and current speed on 19 sigma layers, were gathered from the NCEP Coastal Ocean Forecast System (COFS). These provide the initial field and open boundary conditions for the POM. The horizontal resolution of the COFS data is about 10–20 km in the SAB and the MAB, becoming coarser with distance from shore. Because the COFS assimilates the location of the northern wall of the Gulf Stream as determined from satellite altimetry and SST, it provides a realistic initial condition for our coupled model simulations. Open ocean boundary conditions are fixed during model integration because the open ocean boundaries of the domain are located far from the storm track, and conditions on these boundaries are independent of the storm's forcing. Since the initial condition obtained from the COFS contains the tides, a time-dependent tidal forcing is linearly superimposed along the open boundary. The resultant tidal current is mostly less than a few cm s^{-1} except on Georges Bank, which is far from the impacts of the particular storm discussed in this paper.

3. Synoptic Description of the Case Study

[13] In order to study air-sea coupling under strongly forced conditions of high winds and strong SST gradients,

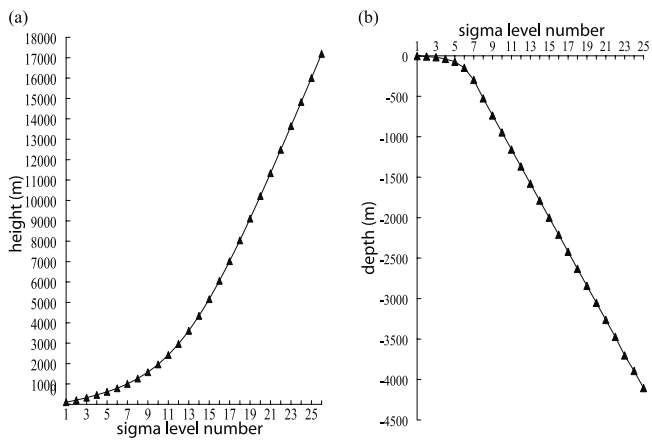

Figure 2. Vertical levels of the (a) ARPS and (b) POM.

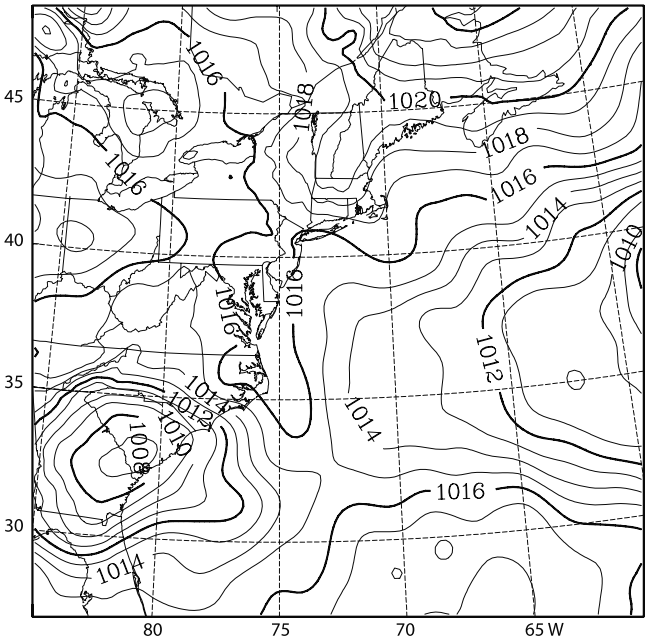

Figure 3. Sea level pressure field from the Eta reanalysis at 12 GMT, 19 January 1998.

we seek to simulate the evolution of an extratropical cyclone. The 19–20 January 1998 storm off the eastern U. S. was selected from the Eta reanalysis, because it exhibits a typical intensification pattern over the Gulf Stream, although it does not meet the explosive development criterion of *Sanders and Gyakum* [1980] (i.e., 1 mb h^{-1} for 24 hours).

[14] This cyclone moved off the Carolina coast in the east-northeast (ENE) direction and developed rapidly. At 12 GMT, 19 January 1998, a weak low-pressure center (1007 mb) was located near the Georgia–South Carolina border (Figure 3). An approaching upper level trough steered the surface low as it moved from the coast. In a period of 24 hours, the cyclone traveled about 1400 km in the ENE direction, and the center pressure dropped by 17 mb (Figure 4).

[15] It is important to note that the reanalysis fields do not match reality exactly, since they are the Eta model's blend of scarce observational data. In addition, the resolution of the reanalysis fields is coarse relative to the sharp gradients associated with the cyclone. However, as model-interpolated observations, the reanalysis fields offer an adequate dataset for validation of the coupled model used in the current study. This comparison is not fully independent, since the initial and boundary conditions for the coupled model also come from the Eta reanalysis. However, the evolution of the coupled model proceeds without further adjustment to the reanalysis fields.

4. Coupled Model Results

[16] The coupled model is used to determine the evolution of the 19–20 January 1998 storm. This evolution includes the collocation of air-sea flux maxima and the Gulf Stream, upper ocean circulation driven by the storm forcing, and a surface wind response to the storm-modified oceanic fields.

4.1. Cyclone Track and Center Pressure

[17] Both the atmospheric model and the oceanic model were initialized at 12 GMT, 19 January 1998, and were simultaneously run forward in time for 24 hours. Figure 4 shows the comparison of cyclone location and center pressure between the coupled model simulation and the Eta reanalysis.

[18] In this case study, a weak surface low moved eastward from inland of the Carolinas and reached the coast near Cape Romain. In the first 6 hours following 12 GMT 19 January 1998, SLP decreased faster in the coupled model simulation than in the Eta reanalysis. By 06 hours (model time), the modeled SLP had dropped 7 mb, while the reanalysis SLP decreased 3 mb. SLP did not change between 06 and 09 hours in either the reanalysis or the simulation. Starting from 09 hours, the tendency of SLP variation was consistent between the reanalysis and the simulation; however, SLP decreased faster in the reanalysis, approximately 1 mb more in every 3 hour increment.

[19] The differences are mostly due to the fact that the Gulf Stream was better resolved in COFS with a tighter SST gradient in the SAB, while a lower resolution, temporally averaged SST field was used in the reanalysis. Spatial and temporal averaging adopted in the reanalysis reduced the SST gradient in the SAB, but increased the gradient farther offshore. As a stronger SST gradient could induce a greater heat flux gradient and hence more rapid deepening of the cyclone, the coupled model showed faster decreases of the center pressure in the first 6 hours over the SAB, but slower

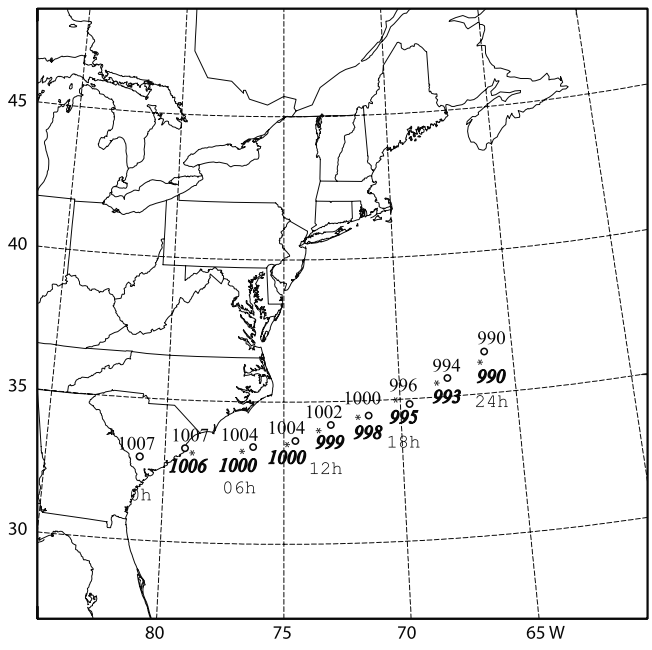

Figure 4. Comparison of the cyclone center position and sea level pressure between the NCEP reanalysis and the coupled-model simulation. Circles denote the cyclone center position from the Eta reanalysis. Pressure from the Eta reanalysis is in regular type. Asterisks and italics denote the model-simulated cyclone center position and pressure.

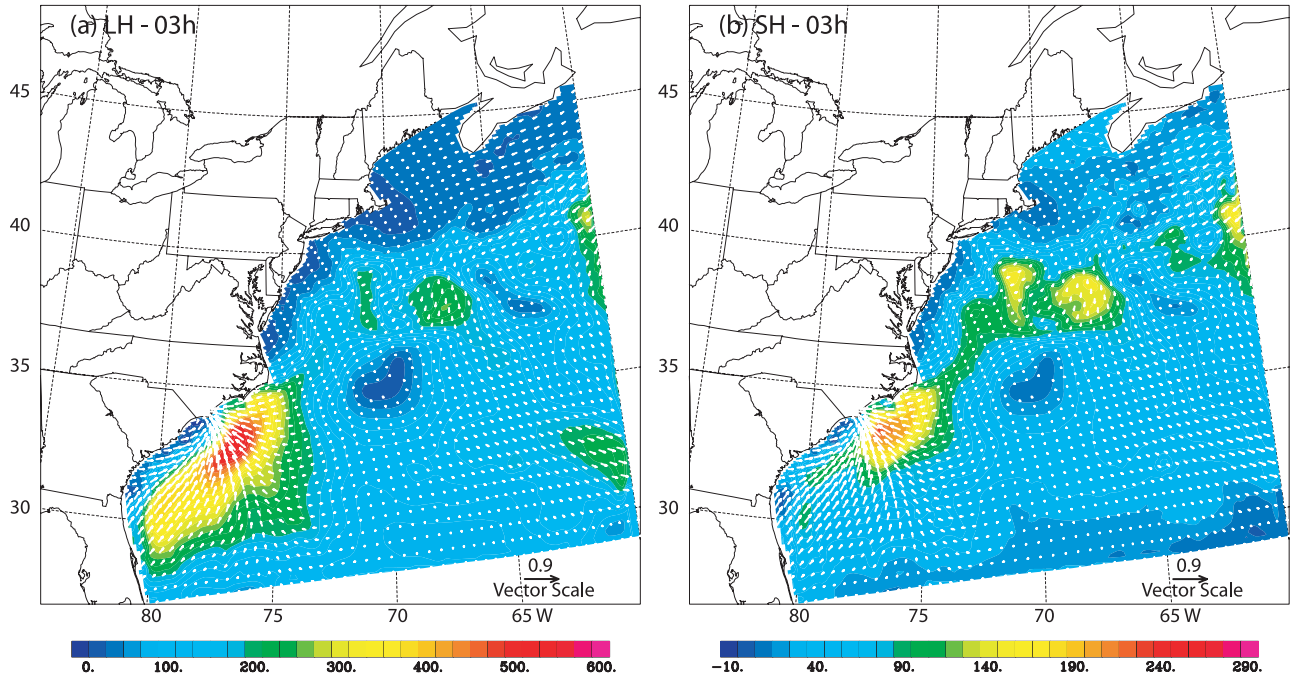

Figure 5. Distributions of (a) latent heat flux and wind stress and (b) sensible heat flux and wind stress at 03 hours. The scales are W m^{-2} for heat fluxes and N m^{-2} for wind stress.

in the later half of the simulation when the cyclone was farther offshore. The center pressure was the same (990 mb) at 24 hours in both the reanalysis and the simulation. The mean departure of the simulated cyclone center position from that of the Eta reanalysis was about 40 km within this 24 hour model integration.

4.2. Heat and Momentum Fluxes

[20] Spatial distributions of the latent heat flux, sensible heat flux and wind stress at 03, 06, 12, and 24 hours of model time are shown in Figures 5, 6, 7, and 8, respectively. At 03 hours the cyclone center was near Cape Romain (Figure 4), and the shelf water and the Gulf Stream in the SAB were under the influence of southwesterly to southeasterly winds. Large heat fluxes appeared along the Gulf Stream in the SAB with a maximum latent heat flux of 575 W m^{-2} and maximum sensible heat flux of 273 W m^{-2} (Figure 5). The relatively low SST of the shelf waters resulted in low heat fluxes there. Small heat fluxes north of Cape Hatteras were due to calm winds there at the time.

[21] At 06 hours the cyclone center had moved from the coastline to the shoreward side of the Gulf Stream in the SAB. It was rather calm over the shelf in the southern SAB, while northeasterly wind prevailed over the northern SAB (Figure 6). Though the winds were weaker, the heat fluxes over the shelf water were larger than those at 03 hours because of the northwesterly flow of colder air behind the cold front. The location of the cold front at this time extended southwestward from the cyclone center along the convergence line between the southwesterly and northwesterly winds. Strongest winds appeared over the Gulf Stream and, correspondingly, large heat fluxes were found over the Gulf Stream under the influence of strong southwesterly wind. Large heat flux gradients occurred along the shoreward side of the Gulf Stream near the center of the cyclone at both 03 and 06 hours. The result was that the cyclone intensified rapidly while the central SLP of the cyclone dropped 6 mb from 03 to 06 hours (Figure 4), similar to observations in earlier storms [e.g., *Wayland and Raman*, 1989; *Riordan*, 1990; *Kuo et al.*, 1991]. Such heat flux gradients could result in baroclinic instability in the MABL, frontogenesis and further storm intensification offshore. As the cyclone moved east-northeastward during this time, the area of high latent and sensible heat fluxes expanded along the Gulf Stream, from the northern SAB to off Cape Hatteras and the southern MAB, where northeasterly wind prevailed in the northern part of the cyclone.

[22] After 06 hours the cyclone moved away from the SAB in the ENE direction. The shelf water and the Gulf Stream in the SAB were under the influence of westerly and northwesterly winds behind the cyclone's cold front. At 12 hours the latent heat flux and sensible heat flux over the Gulf Stream in the SAB decreased (Figure 7) relative to those at 06 hours. This was because the wind speeds at 12 hours were smaller than those at 06 hours in this area, although air-sea temperature differences were larger and humidity differences were favorable for evaporation. The largest latent heat flux (~410 W m^{-2}) and sensible heat flux (~265 W m^{-2}) at 12 hours were located over the Gulf Stream off Cape Hatteras in the area dominated by northeasterlies. The ratio between latent heat flux and sensible heat flux decreased due to the higher humidity carried by the northeasterly wind, and this reduced evaporation from the sea surface.

[23] At 24 hours the cyclone was far away from the coast. Heat fluxes were relatively large on the northern limb of the cyclone; however, the heat flux maximum occurred east of Cape Hatteras and near the shelf break of the MAB where northerly winds brought dryer, colder air (Figure 8). As a

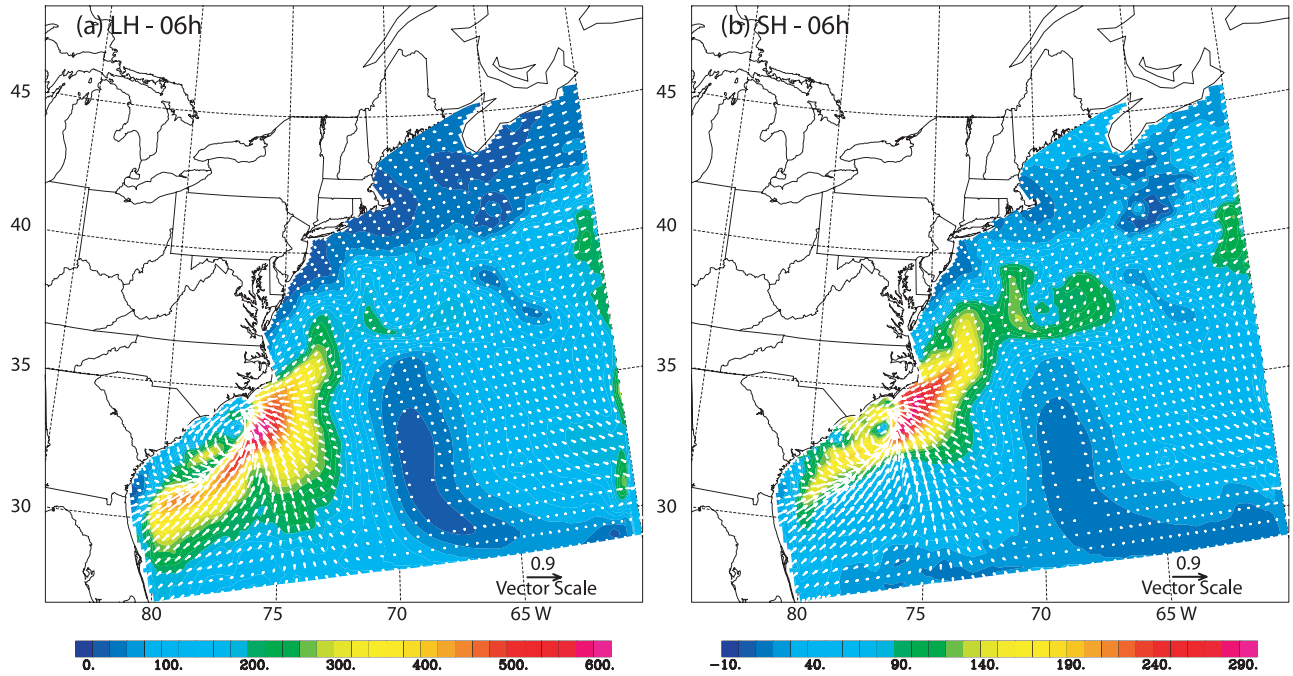

Figure 6. Similar to Figure 5 but at 06 hours.

result, surface winds were locally enhanced in the area of heat flux maximum.

4.3. Modification of the Upper Ocean

4.3.1. Surface Currents

[24] Surface currents were estimated at the first sigma level. For a water column depth of 4000 m, the first sigma level is located about 3 m below the sea surface. Wind-driven currents were most apparent on the shelf except on Georges Bank where large velocities were mostly tidally driven. At 03 hours, which was before the cyclone center moved off the Carolina Coast, the shelf water in the SAB flowed northward and onshore following the wind direction (Figure 9a). At 06 hours a cyclonic eddy appeared over the shelf and slope south of Cape Hatteras (Figure 9b), coincident with the cyclonic winds seen in Figure 6.

[25] At 12 hours (Figure 9c) the surface flow of the Gulf Stream in the SAB decreased as a result of southward

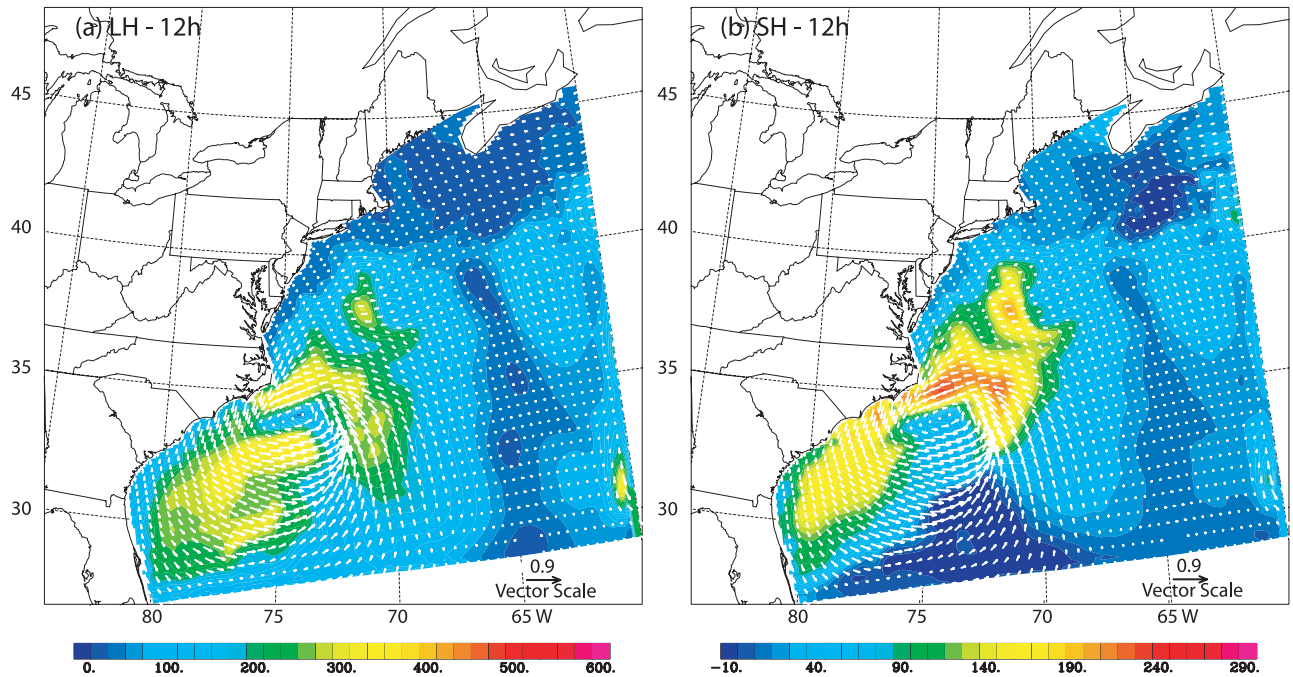

Figure 7. Similar to Figure 5 but at 12 hours.

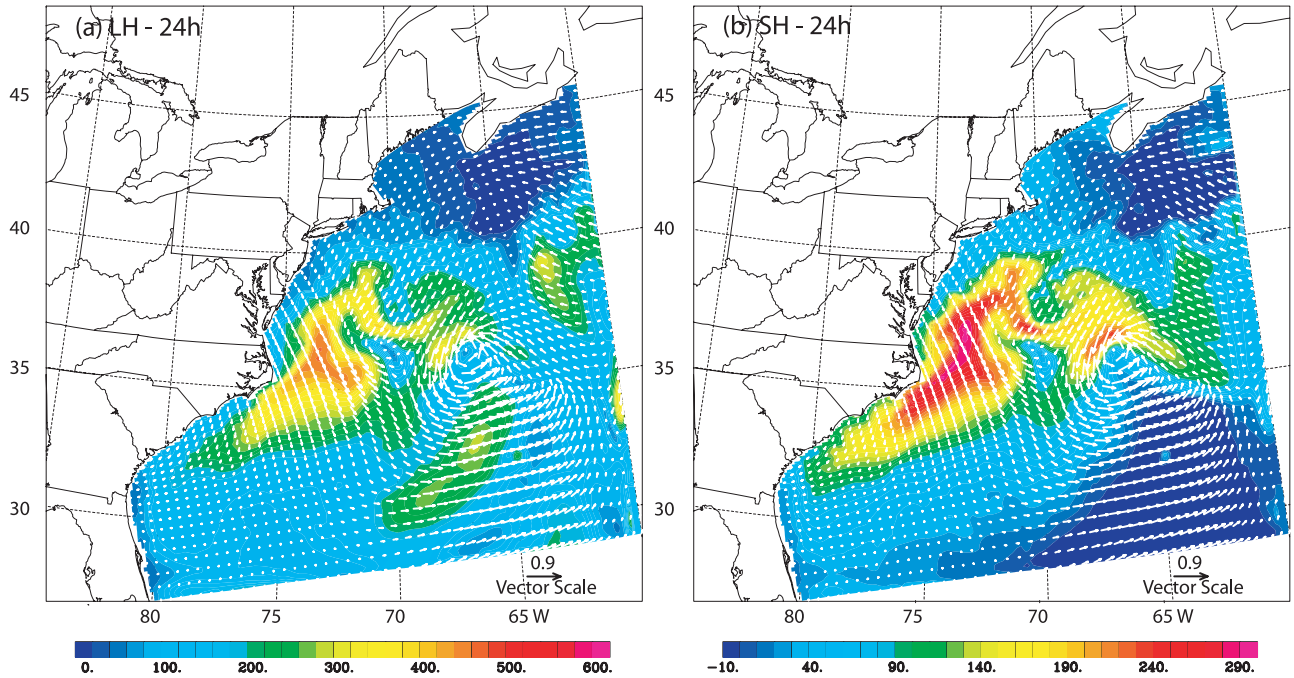

Figure 8. Similar to Figure 5 but at 24 hours.

Ekman drift induced by the northwesterly wind behind the atmospheric cold front. This caused a portion of the Gulf Stream to turn offshore and flow toward the Sarggaso Sea. Furthermore, an extensive southwestward shelf current appeared, stretching from Virginia, past Cape Hatteras to Cape Roman. This shelf current was strongest off Cape Fear. Under the influence of northeasterly wind, the Gulf Stream off Cape Hatteras had a tendency to move onshore, and an effluence from the Gulf Stream brought warm water to the shelf, resulting in an increased SST in the southern MAB (see discussion later). Moreover, the onshore movement of the Gulf Stream also resulted in an increase in the surface current speeds off Cape Hatteras and along the shelf break in the MAB.

[26] At 24 hours, an almost enclosed cyclonic eddy appeared south of the Gulf Stream in Sargasso Sea, centered underneath the atmospheric cyclone. Surface currents in the SAB rebounded toward their precyclone condition when the cyclone moved away from this area. The flow across the shelf break remained onshore in the southern MAB, although the wind was predominantly offshore at the time. The reason is that northwesterly wind prevailed over the southern MAB starting from 16 hours, which drove the coastal water southeastward. Since the Gulf Stream was within 20 km from the shelfbreak, much of the southward moving coastal water was unable to round Cape Hatteras, and instead, was steered back northward to strengthen the Gulf Stream north of Cape Hatteras. Meanwhile, the wind was predominantly from the northeast over the northern MAB, and the surface flow in that part of the Gulf Stream decreased. The increased (decreased) surface current to the south (north) resulted in the onshore flow across the shelf break. Shoreward flow in this location is infrequent in the real ocean, but has been observed on occasion [*Savidge and Bane*, 2001].

[27] To further illustrate the oceanic response to this cyclone, downstreamflow in the upper 500 m at sections A, B, and C (see Figure 9a) are shown in Figures 10, 11, and 12, respectively. Positive values point along the Gulf Stream (i.e., into the page). Negative values point upstream and are shaded. When the SAB was under the control of southerly wind at 03 hours, the shelf flow was strongly northward, reaching 0.6 m s^{-1} at the surface. Meanwhile, the Gulf Stream's surface velocity increased in the downstream direction, and surface water from the Stream was driven offshore. The cyclonic shear side of the stream was constrained horizontally and the anticyclonic shear side spread well offshore. Because of northerly and northwesterly winds behind the cold front at 12 hours, a strong southwestward current had appeared on the shelf and the upper slope by then. The Gulf Stream's surface downstream velocity had decreased, and the maximum speed appeared at about 130 m below the surface. The southward velocity on the Sargasso Sea side of the stream had increased in the upper 100 m. From 12 to 24 hours, winds gradually diminished as the storm moved away from the SAB, the southward flows on the shelf and farther offshore decreased, and the Gulf Stream jet maximum began to return to the surface.

[28] Modification near Cape Hatteras (Figure 11) was somewhat different. At 03 hours winds were light near Cape Hatteras and the Gulf Stream's maximum downstream velocity was at the surface, at about 1.7 m s^{-1}. From 03 to 12 hours, the Stream was driven onshore by the northeasterly winds. Its downstream velocity was strengthened and the maximum downstream speed of 1.9 m s^{-1} appeared at about 50 m below the surface. Though considerably weaker, the southward shelf current seen at section A (Figures 10b and 10c) was also present at section B. This southward flow broke through the usual constriction at Cape Hatteras and

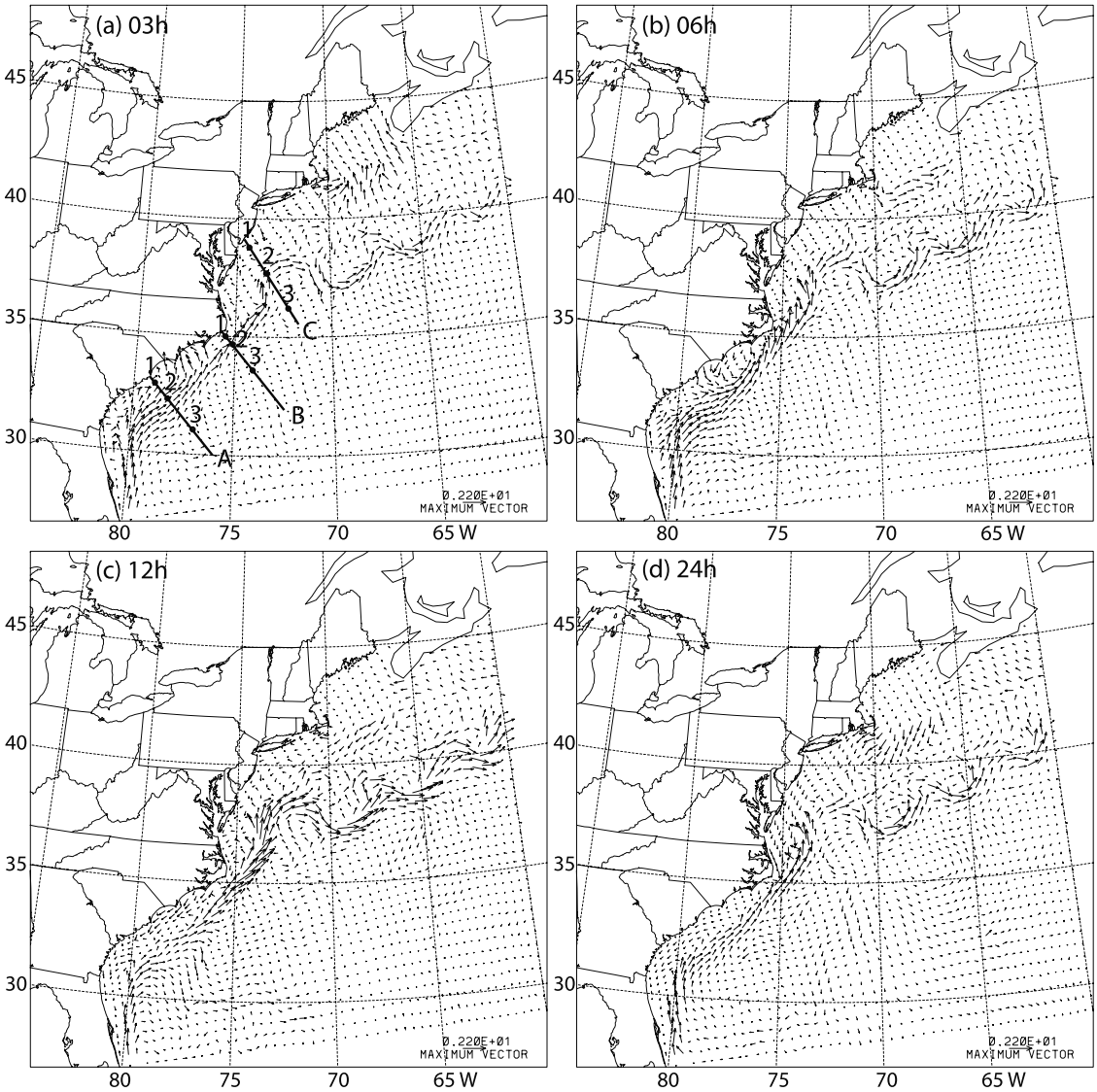

Figure 9. Surface current in m s^{-1} at (a) 03, (b) 06, (c) 12, and (d) 24 hours. Three sections and three stations on each section are highlighted in Figure 9a for use in subsequent figures showing oceanic responses in the SAB (section A), off Cape Hetteras (section B), and in the MAB (section C) and on the shelf (1 s), in the Gulf Stream (2 s), and in the open ocean (3 s).

allowed MAB shelf water to invade the SAB at this time. There was an increase in the southward flow to the east of the Gulf Stream. Although the maximum speed of 0.4 m s^{-1} occurred at the surface, southward flow of 0.2 m s^{-1} could reach the thermocline depth.

[29] At section C (Figure 12), the downstreamflow in the Gulf Stream strengthened from 03 to 12 hours. Both its magnitude and width increased. The southwestward flow east of the Gulf Stream also increased slightly. By 24 hours, the northeasterly wind forced the flow such that the southwestward currents on the shelf and east of the Gulf Stream were enhanced, the surface velocity in the Gulf Stream had reduced, and the Stream's velocity maximum appeared below the surface. Note that even at the 500 m level, velocity varied by 0.2 m s^{-1}, in contrast to the 2D coupled model results of *Xue et al.* [2000] in which velocity variations were limited to the mixed layer. The reason is that the downstream gradient, which is necessarily ignored in 2D models, generated areas of convergence and divergence at the base of the mixed layer, which in turn modified the flow field below the mixed layer.

4.3.2. Sea Surface Temperature

[30] Two factors that determine temporal variations of the SST are storm-associated cooling and lateral water movements. Gulf Stream waters that are driven by storm winds are especially effective at transporting heat and modifying SST. Various stations representing the shelf water, the Gulf Stream and the open ocean in the SAB, off Cape Hatteras and in the MAB (see Figure 9a) were selected to illustrate the SST response. SST time series from these stations are shown in Figure 13. Over the shelf in the SAB (station A_1) SST increased during the first 5 hours and then decreased by about 1.5°C from 06 to 24 hours. At station B_1 (adjacent to Cape Hatteras) SST decreased from 22° to 21°C in the first 7 hours and then quickly increased to nearly 23°C between 07 and 12 hours, which was followed by another decrease

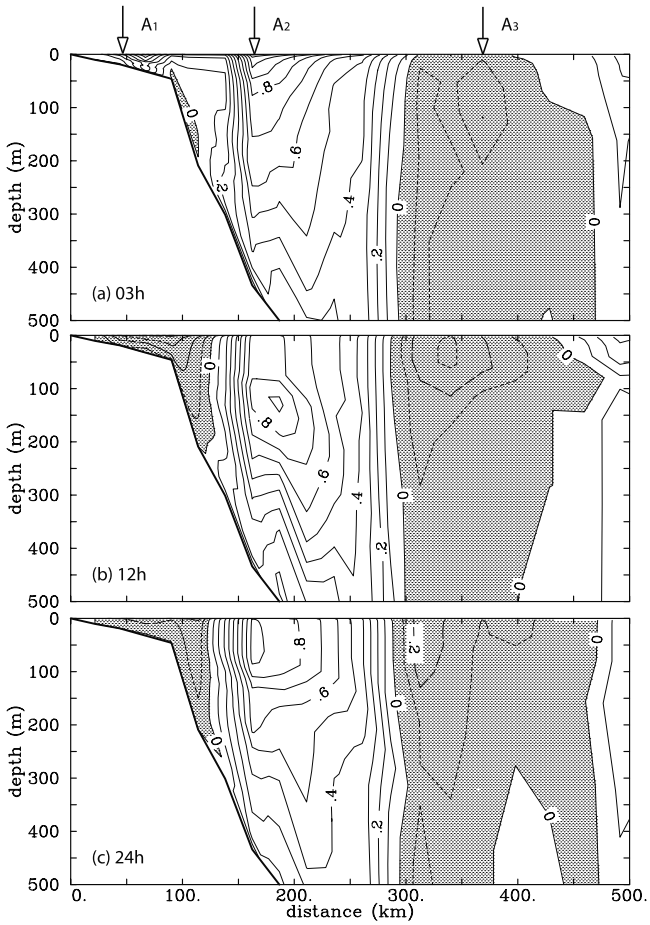

Figure 10. Downstream velocity at section A at (a) 03, (b) 12, and (c) 24 hours. Shaded areas correspond to southwestward flows, opposite to the downstream direction of the Gulf Stream.

of about 2°C in the next 10 hours. At station C_1 (MAB shelf) SST first increased and then decreased after 07 hours.

[31] Diagnostic calculation of the thermodynamic equation suggested that at station A_1 oceanic heat loss to the atmosphere (S&L) was the dominant term, which was partially compensated by the heat pumped from the water column below the surface (H_b) (Figure 14a). However, the increase of SST in the first 5 hours was due to northward transport of warmer water driven by the southerly wind ($H_y > 0$ and $H_x > 0$) as suggested by the positive downstream velocity at station A_1 in Figure 10a. The subsequent decrease between 06 and 24 hours was due to the combined effect of invading cold water from the north (again consistent with the negative downstream velocity at station A_1 in Figures 10b and 10c) and greater heat loss across the sea surface under the influence of cold northwesterly wind. A different heat balance was found at station B_1 (Figure 14b), where the lateral heat transport (mostly H_y) dominated due to the proximity of the Gulf Stream. H_y was largely compensated by the vertical heat transport (H_b). It was clear that the SST increase between 07 and 12 hours resulted from onshore movement of the Gulf Stream while the subsequent decrease resulted from persistent cooling and southwestward shelf flows. Although the net heat gain (SUM) was the small difference of several large terms and might be contaminated by numerical errors, its tendency was reasonably consistent with the temporal variation of the SST. Station C_1 was similar to station A_1, where the oceanic heat loss to the atmosphere (S&L) was the dominant term (Figure 14c). The increase in the first 7 hours resulted from the intruding warm Gulf Stream water onto the shelf, while the subsequent decrease could be attributed to increased cooling associated with the cold and dry northwesterly wind.

[32] Variation of the surface temperature in the Gulf Stream during the 24 hour integration is shown in Figure 13b. In the SAB (station A_2) SST decreased from 06 hours until the end of model integration due to the influence of cold air behind the cold front, while offshore (station A_3) and downstream of Cape Hatters (station C_2) it changed very little before 18 hours, although the wind was predominantly northeasterly from 09 to 18 hours. This is due to in the relatively warm and moist oceanic air carried by the northeasterly wind, resulting in a weak heat loss. Additionally, the swift Gulf Stream carried warmer water from the south to help compensate for the heat loss. After 18 h the Gulf Stream surface temperature off Cape Hatters (station B_2) and near the shelf break in the MAB (station C_2) decreased because of stronger heat loss from the sea surface during northwesterly wind. SST variations in the open ocean were smaller than those in the shelf water and in

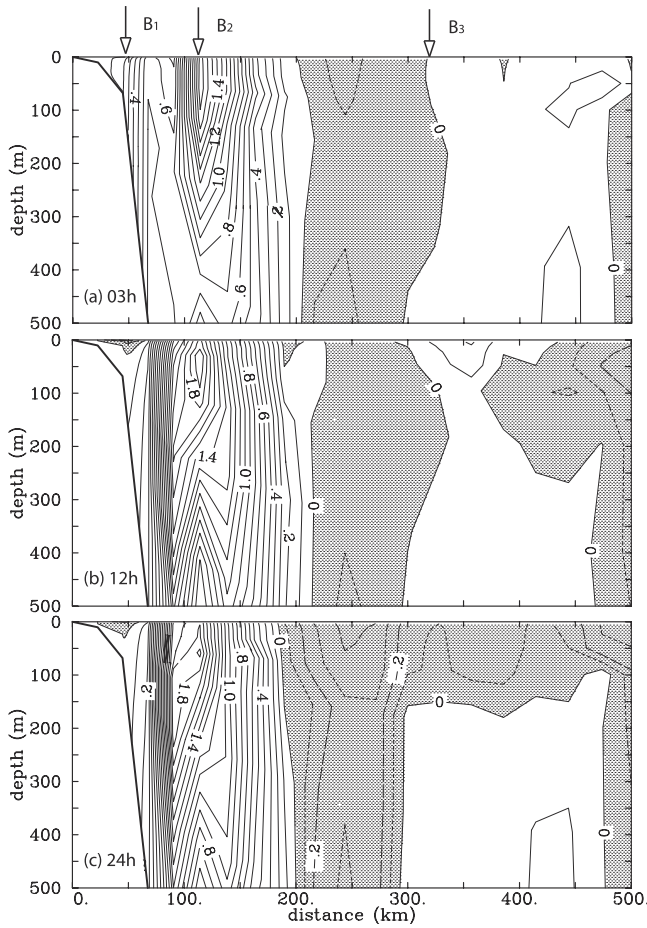

Figure 11. Similar to Figure 10 but for section B.

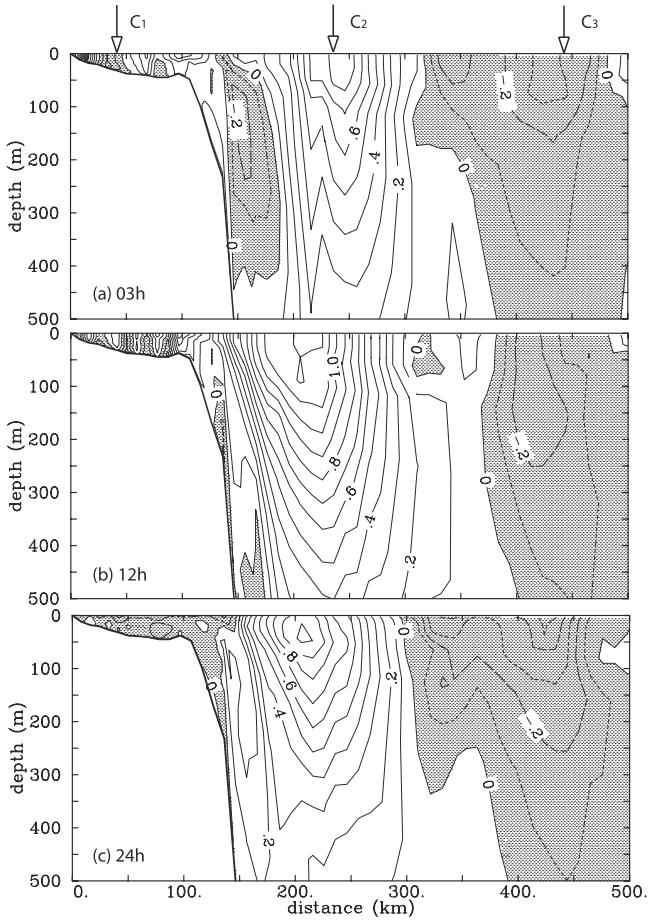

Figure 12. Similar to Figure 10 but for section C.

the Gulf Stream, no more than 0.1°C during the 24 hour integration period (Figure 13c).

4.3.3. Effects of Air-Sea Coupling

[33] Many mesoscale atmospheric models use an unchanged sea surface condition (e.g., the monthly climatological SST) during model integration. When a fixed SST is used, the atmospheric response to a more realistic, temporally and spatially varying SST field cannot be addressed. Generally speaking, the feedback from the changing SST would be small for fast moving synoptic systems [*Hodur and Doyle*, 1999; *Xue et al.*, 2000], but the precise effects of such feedbacks have been unknown. To estimate this feedback quantitatively, another experiment was carried out, in which the oceanic model always conveyed the initial SST to the atmospheric model even though SST in the oceanic model varied with time. All other conditions were the same in the two experiments. This experiment, designated the ''forced experiment,'' is equivalent to running two forced models simultaneously such that the atmospheric model is forced with a fixed SST and the oceanic model is forced with time varying heat and momentum fluxes from the atmospheric model that is forced by a fixed SST.

[34] Differences in the surface heat fluxes (latent and sensible) and wind stress between the coupled experiment and the forced experiment at 12 and 24 hours are shown in Figure 15. The heat flux difference ranged from −30 to 150 W m^{-2}. If taking a one-dimensional view, the heat flux should be smaller in the coupled experiment (negative anomaly) since continuous heat loss would lower the SST and hence reduce the air-sea temperature contrast. This seemed to be the case in a large part of the domain, where the heat flux difference was negative, about −5 W m^{-2} at 12 hours and −20 W m^{-2} at 24 hours, or 2 and 4% of the total heat flux at the time, respectively. The ocean surface is, however, not stationary, and lateral shifts of the Gulf Stream can change the SST more dramatically than can direct heat loss to the atmosphere. This is seen at station B_1 in Figure 13a where the onshore movement of the Gulf Stream resulted in an increase of SST from 07 to 13 hours. Therefore, the heat flux difference was positive near Cape Hatteras. The positive values were far greater than the negative ones, on the order of 150 W m^{-2}, i.e., about 20% of the total heat flux. Similarly, a large heat flux difference was found near the Gulf Stream front around 69°W (a meander trough was in that region, as seen in Figure 9). Smaller positive heat flux differences were found near the Gulf Stream front at meander crests where the

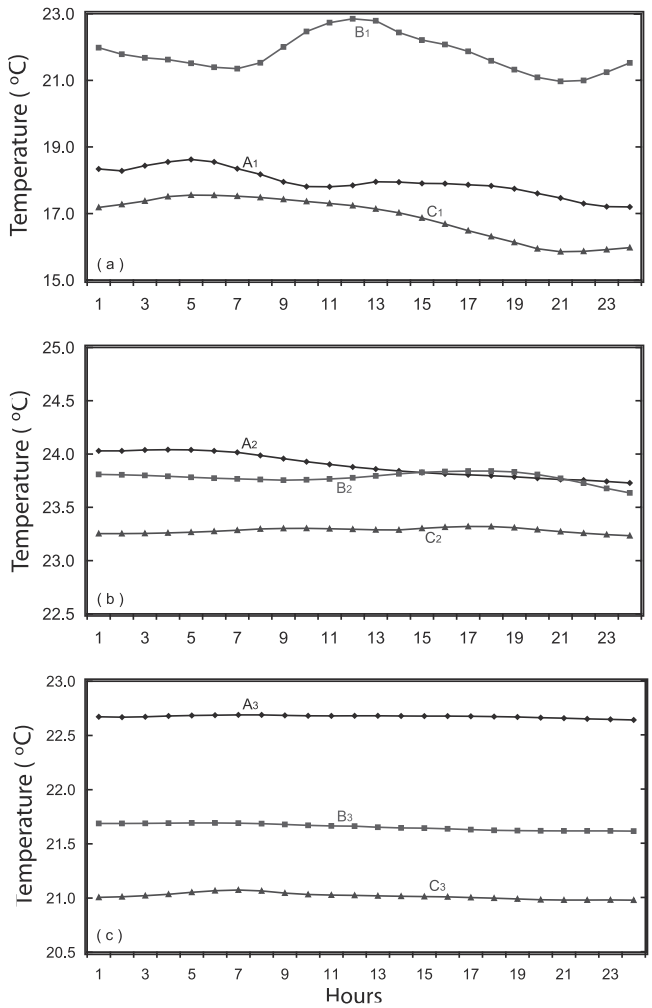

Figure 13. SST time series representing (a) the shelf waters, (b) the Gulf Stream, and (c) the open ocean. See Figure 9a for station locations (A_1, B_1, etc.).

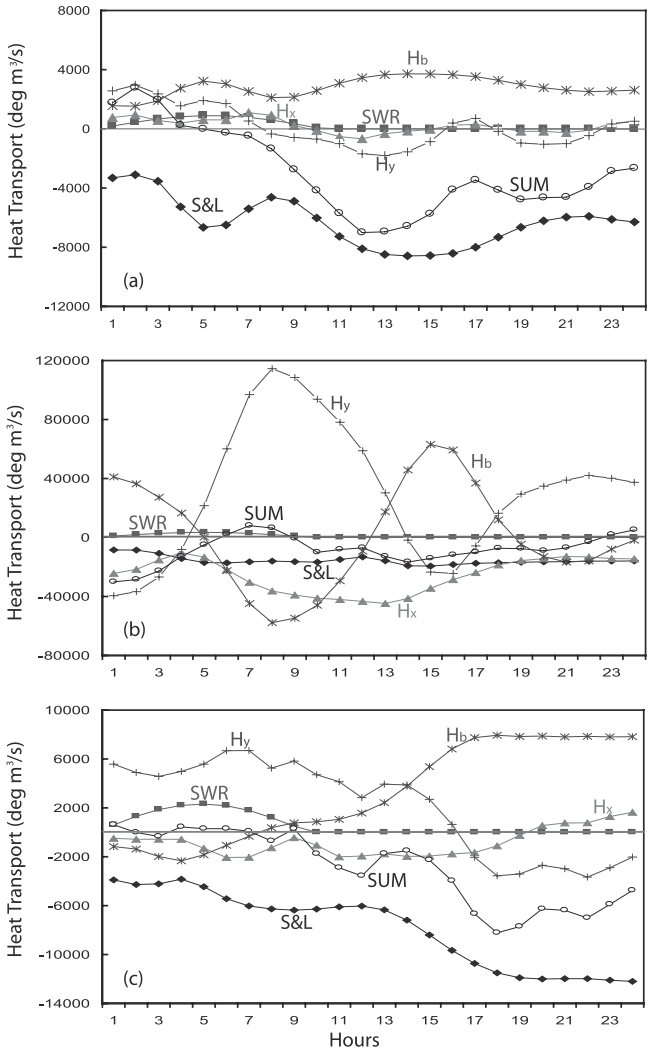

Figure 14. Diagnostic estimates of heat transports at (a) station A_1, (b) station B_1, and (c) station C_1. A single grid cell control volume (dx × dy × Ddσ) was used at each station. SUM = S&L + SWR + H_x + H_y + H_b, and positive (negative) represents net heat gain (loss). S&L = sensible and latent heat transport from the atmosphere to the ocean; SWR = absorption of the shortwave radiation by the surface layer (this term was relatively small in the rather thin surface layer); H_x = net heat transport in the x direction; H_y = net heat transport in the y direction; and H_b = net heat transport through the bottom of the surface layer. H_x, H_y, and H_b included both the advection and diffusion. Although not shown separately, horizontal diffusion was negligible, but vertical diffusion contributed to H_b significantly. Finally, note that x and y were the locally orthogonal coordinates.

temperature gradients were not as strong as those at meander troughs.

[35] The greatest differences in wind stress between the coupled and forced experiments were located near the center of the cyclone (designated as L in Figure 15) and near the Gulf Stream. The differences around the cyclone center increased from 0.02 N m^{-2} at 12 hours to 0.05 N m^{-2} at 24 hours. The latter was nearly 10% of the local wind stress at the time (Figure 8). Taking into account the rotating wind associated with the cyclone, it is clear that the cyclone wind speed in the coupled experiment was smaller than that in the forced experiment. Due to lower SST in the coupled experiment compared with the forced experiment, smaller latent and sensible heat losses from the ocean to the atmosphere occurred. In general, the more heat gain by the atmosphere, the stronger the cyclone. In the vicinity of the Gulf Stream, winds were enhanced/reduced in the areas of positive/negative heat flux differences, respectively.

[36] Figure 16 shows the differences in the ocean surface current between the coupled and the forced experiment. The magnitude and direction of the anomalies were consistent with the differences in wind stress between the two experiments seen in Figure 14. Although the wind stress and heat fluxes changed only small percentages, the ocean surface current differed from a few cm s^{-1} to as much as 10 cm s^{-1}, which were significant variations of the current on the shelf and in the open ocean.

5. Summary

[37] The three-dimensional ARPS was coupled with the POM to investigate air-sea interactions off the east coast of North America during a winter storm passage over the northwestern Atlantic. The extratropical cyclone that developed and moved off the Carolina coast on 19–20 January 1998 was selected as a case study. When initialized with the atmospheric conditions from the NCEP Eta reanalysis and the oceanic condition from the COFS simulation, the coupled model simulated well the cyclone's path and central pressure.

[38] Cyclones like this provide some of the strongest meteorological forcing for the ocean. In this paper, model diagnoses are used to examine air-sea heat and momentum exchanges and velocity responses in the upper ocean, based on a 24 hour coupled model simulation. Heat fluxes were always larger over the Gulf Stream than other areas during the storm's passage. Maximum latent and sensible heat fluxes appeared over the Gulf Stream in the SAB and extended northeastward following the southwesterly wind before the cyclone's cold front reached the Gulf Stream. Strong lateral gradients in latent and sensible heat fluxes resulted in rapid deepening of the cyclone, about 6 mb of central pressure decrease within 3 hours during the period that the cyclone center moved from the coastline to the shoreward edge of the Gulf Stream. The heat flux maximum shifted from the SAB to off Cape Hatteras and then to the area northeast of Hatteras as the storm moved away from the coast in the ENE direction. This progression was closely related to wind speed and direction. The latent heat flux resembled the sensible heat flux in spatial distribution but was about 1–2 times larger, and the latent/sensible heat flux ratio decreased in the areas where northeasterly winds dominated.

[39] The oceanic response varied from place to place and, in general, was closely related to the local wind direction at any given time. Given the path of the cyclone (see Figure 4), the wind in the SAB changed from southwesterly to northwesterly and then to northerly. As a result, the shelf flows changed direction from northward to southward, and

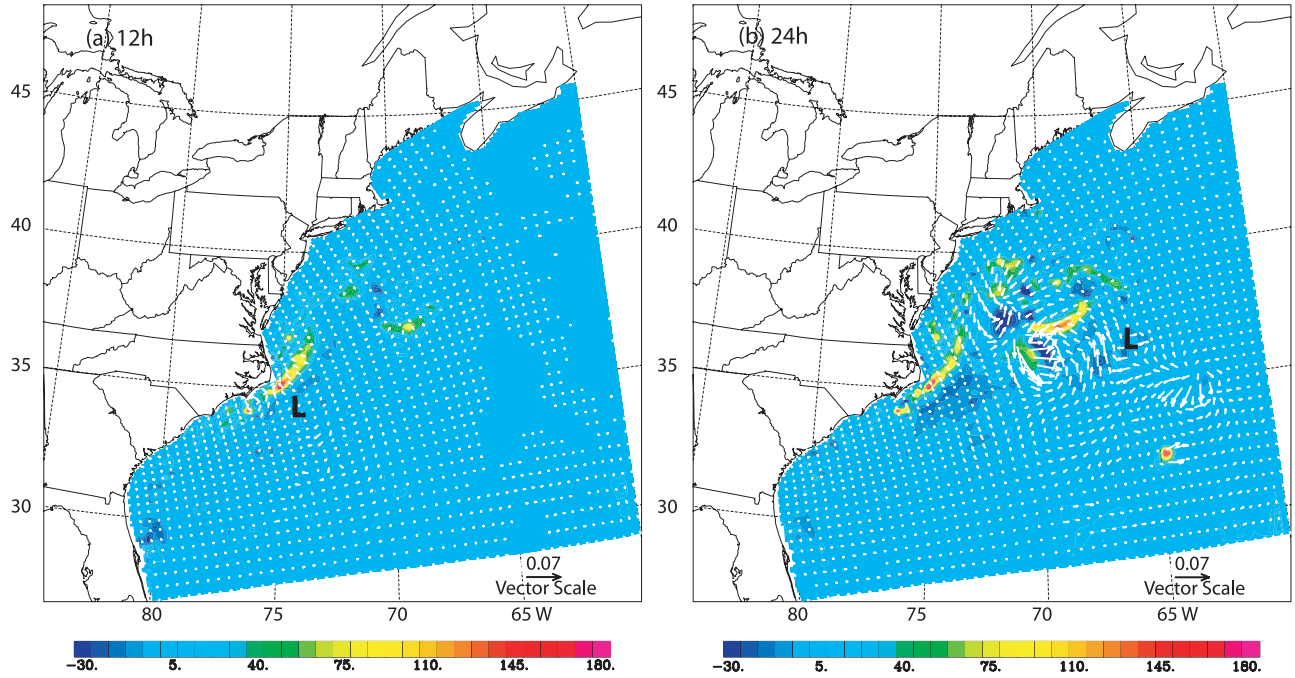

Figure 15. Differences in the total surface heat flux and wind stress between the coupled experiment and the forced experiment at (a) 12 and (b) 24 hours. Units are W m^{-2} for heat flux differences and N m^{-2} for wind stress differences. The white line shows the Gulf Stream's path, and the L denotes the cyclone center location.

the Gulf Stream at first accelerated, then slightly decelerated. Northeasterly and northerly winds controlled the area from Cape Lookout northward, which forced an onshore shift of the Gulf Stream near Cape Hatteras and southward shelf flows in the MAB. SST responded to the storm forcing in two ways: directly to the storm-associated cooling and indirectly to water movements driven by storm winds. In the SAB SST increased at first due to northward transport of warmer water driven by the southerly wind, and then it was followed by a steady decrease under the influence of northerly to northwesterly wind after the cold front had swept over this area. In contrast, SST off Cape Hatteras decreased initially due to surface heat loss. The subsequent increase resulted from onshore movement of the Gulf

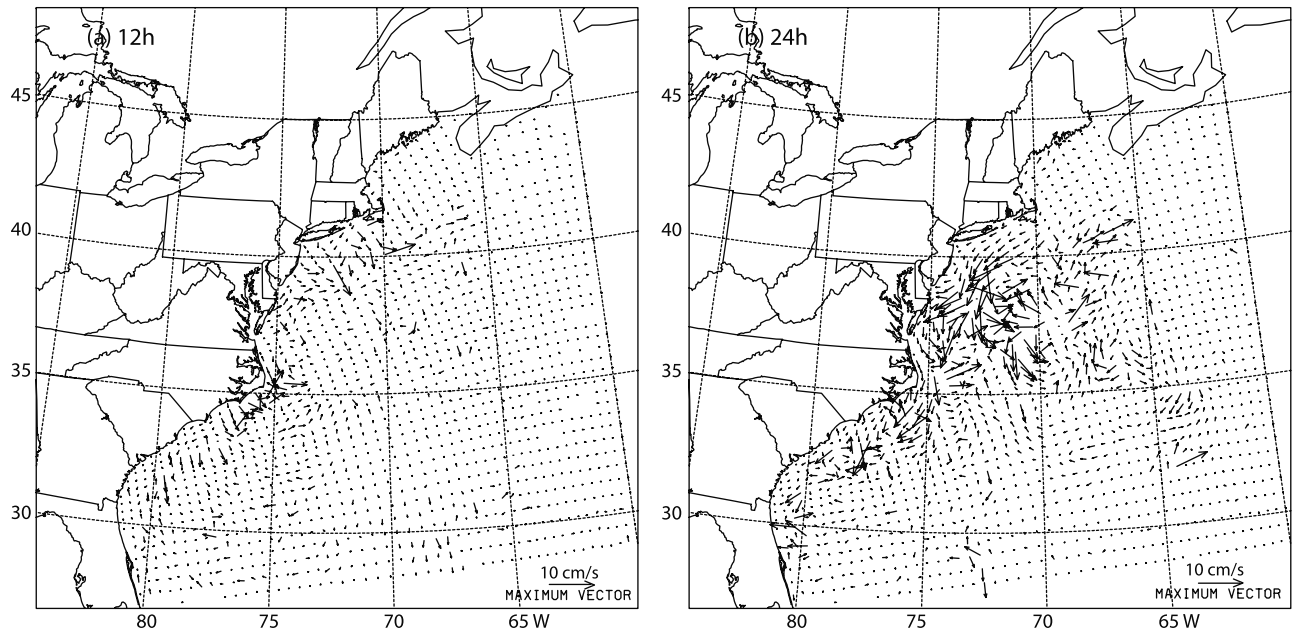

Figure 16. Differences in the ocean surface current between the coupled experiment and the forced experiment at (a) 12 and (b) 24 hours.

Stream. Variation of the SST in the Gulf Stream and in the open ocean was almost negligible except in the SAB where the surface Gulf Stream lost a considerable amount of heat, and the surface temperature decreased by almost 0.5°C under the influence of northerly to northwesterly winds.

[40] The coupled-model approach was used in this study. It is of particular interest to investigate when and where feedback between the atmosphere and the ocean plays a role, and to determine how important the feedback is. Comparisons between the coupled experiment and the experiment with a fixed SST suggest that the latter overestimates the oceanic impact on the cyclone, for example, the surface wind stress was about 5 $\sim$ 10% stronger than that in the coupled model. The reason was explained by *Xue et al.* [2000], is as follows: heat loss from the ocean in the coupled model continuously lowers the SST, and the decrease in SST is more in the Gulf Stream; thus, not only is less heat lost from the ocean to the atmosphere in the coupled model, but also the heat flux gradient weakens, and consequently a weaker storm develops. This essentially one-dimensional view is not valid near the Gulf Stream where wind-driven lateral movements of the Gulf Stream (especially near meander troughs where sharp fronts are found) changed the SST more dramatically than the surface cooling. This resulted in increases in total surface heat flux in the coupled experiment by as much as 20%. These positive heat flux anomalies helped to maintain the relatively strong northeasterly winds over the MAB after the storm moved out over the open ocean. The ocean surface current differed by as much as 10 cm s^{-1} between the coupled experiment and the experiment in which the oceanic model is forced with time varying heat and momentum fluxes from the atmospheric model forced by a fixed SST, which were significant variations of the current on the shelf and in the open ocean. The magnitude and the direction of the velocity differences were consistent with the wind stress anomaly in these two experiments.

[41] The storm on 19 January 1998 was not particularly severe. Feedbacks are likely to be stronger during severe winter storms, especially slowly moving ones. Furthermore, when winter storms quickly move through this region, temporal variation should be expected at any fixed point observation. Note that the scale of the wind field is smaller than the N-S scale of the eastern seaboard. Alongshore gradients in the oceanic response cannot be ignored as was done in the 2D studies of *Chao* [1992] and *Xue et al.* [2000]. Fixed point observations should be viewed coherently in the process of moving storms. For example, it appears that the occurrence of the southwestward shelf flows is consistent with the timing when the northeasterly wind becomes predominant in the SAB, off Cape Hatteras, and in the MAB, respectively. The type of transient response from the south to the north should be further investigated with concerted modeling and observational efforts when a consortium of east coast observing systems becomes reality.

[42] **Acknowledgments.** This work was supported by the National Science Foundation through grants to the University of Maine and the University of North Carolina at Chapel Hill. Computational support was provided by the North Carolina Supercomputing Center. Also, we thank the two thorough and helpful referees for thoughtful comments and suggestions.

References

Ademec, D., and R. L. Elsberry, Numerical simulations of the response of intense ocean currents to atmospheric forcing, *J. Phys. Oceanogr.*, *15*, 273–287, 1985a.

Ademec, D., and R. L. Elsberry, The response of intense oceanic current systems entering regions of strong cooling, *J. Phys. Oceaongr.*, *15*, 1284–1295, 1985b.

Beardsley, R. C., and B. Butman, Circulation on the New-England continental shelf: Response to strong winter storms, *Geophys. Res. Lett.*, *1*, 181–184, 1974.

Blanton, J. O., T. N. Lee, L. P. Atkinson, J. M. Bane, A. J. Riordan, and S. Raman, Oceanographic studies during project GALE, *Eos Trans. AGU*, *68*, 1626–1627, 1636–1637, 1987.

Blanton, J. O., J. A. Amft, D. K. Lee, and A. Riordan, Wind stress and heat fluxes observed during winter and spring 1986, *J. Geophys. Res.*, *94*, 10,686–10,698, 1989.

Blumberg, A. F., and G. L. Mellor, A description of a three-dimensional coastal ocean circulation model, in *Three-Dimensional Coastal Ocean Models, Coastal Estuarine Sci.*, vol. 4, edited by N. Heaps, pp. 1–17, AGU, Washington, D.C., 1987.

Businger, J. A., J. C. Wyngaard, Y. Izumi, and E. F. Bradley, Flux-profile relationships in the atmospheric surface layer, *J. Atmos. Sci.*, *28*, 181–189, 1971.

Chao, S.-Y., An air-sea interaction model for cold air outbreaks, *J. Phys. Oceanogr.*, *22*, 821–841, 1992.

Dirks, R. A., J. P. Kuettner, and J. A. Moore, Genesis of Atlantic Lows Experiment (GALE): An experiment, *Bull Am. Meteorol. Soc.*, *69*, 148–160, 1988.

Hadlock, R., and C. W. Kreitzberg, The Experiment on Rapid Intensifying Cyclones over the Atlantic (ERICA) field study: Objective and plans, *Bull. Am. Meteorol. Soc.*, *69*, 1309–1320, 1988.

Hodur, R. M., and J. D. Doyle, The Coupled Ocean/Atmosphere Mesoscale Prediction System (COAMPS), in *Coastal Ocean Prediction, Coastal Estuarine Ser.*, vol. 56, edited by C. N. K. Mooers, pp. 125–155, AGU, Washington, D.C., 1999.

Kuo, Y.-H., R. J. Reed, and S. Low-Nam, Effects of surface energy fluxes during the early development and rapid intensification stages of seven explosive cyclones in the western Atlantic, *Mon. Weather. Rev.*, *119*, 457–476, 1991.

Mellor, G. L., and T. Yamada, Development of a turbulence closure model for geophysical fluid problems, *Rev. Geophys.*, *20*, 851–875, 1982.

Reed, R. J., G. A. Grell, and Y.-H. Kao, The ERICA IOP 5 storm, part II, Sensitivity tests and further diagnosis based on model output, *Mon. Weather Rev.*, *121*, 1595–1612, 1993.

Riordan, A. J., Examination of the mesoscale features of the GALE coastal front of 24–25 January 1986, *Mon. Weather Rev.*, *118*, 258–282, 1990.

Sanders, F., and J. R. Gyakum, Synoptic-dynamic climatology of the "bomb," Mon, *Weather Rev.*, *108*, 1589–1606, 1980.

Savidge, D. K., and J. M. Bane, Wind and Gulf Stream influences on alongshelf transport and off-shelf export at Cape Hatteras, North Carolina, *J. Geophys. Res.*, *106*, 11,505–11,527, 2001.

Stewart, R. E., R. W. Shaw, and G. A. Isaac, Canadian Atlantic Storms Program: The meteorological field project, *Bull. Am. Meteorol. Soc.*, *68*, 338–345, 1987.

Warner, T. T., M. N. Lakhtakia, J. D. Doyle, and R. A. Pearson, Marine atmospheric boundary layer circulations forced by Gulf Stream sea surface temperature gradients, *Mon. Weather Rev.*, *118*, 309–323, 1990.

Wayland, R., and S. Raman, Mean and turbulent structure of a baroclinic marine boundary layer during the 28 January 1986 cold air outbreak (GALE 86), *Boundary Layer Meteorol.*, *48*, 227–254, 1989.

Xue, H., J. M. Bane Jr., and L. M. Goodman, Modification of the Gulf Stream through strong air-sea interaction in winter: Observations and numerical simulation, *J. Phys. Oceannogr.*, *25*, 533–557, 1995.

Xue, H., Z. Pan, and J. M. Bane Jr., A 2D coupled atmosphere-ocean model study of air-sea interactions during a cold air outbreak over Gulf Stream, *Mon. Weather Rev.*, *128*, 973–996, 2000.

Xue, M., K. K. Droegemeier, V. Wang, A. Shapiro, and K. Brewster, Advanced Regional Prediction System User's Guide, 380 pp., Univ. of Oklahoma, Norman, 1995.

J. M. Bane, Department of Marine Sciences, University of North Carolina, Chapel Hill, NC 27599-3300, USA.

Y. Li, Shanghai Typhoon Institute, 166 Puxi Road, Shanghai, China 200030.

H. Xue, School of Marine Sciences, University of Maine, Orono, ME 04469-5741, USA. (hxue@maine.edu)